CORK BASED THERMAL PROTECTION SYSTEM FOR SOUNDING ROCKET APPLICATIONS – DEVELOPMENT AND FLIGHT TESTING

Oliver Drescher[(1)], Marcus Hörschgen-Eggers[(2)], Grégory Pinaud[(3)], Maxime Podeur[(4)]

[(1)] *Deutsches Zentrum für Luft- und Raumfahrt (DLR)/Oberpfaffenhofen, Mobile Raketen Basis, Münchener Straße 20, 82234 Weßling, Germany, E-mail: oliver.drescher@dlr.de*

[(2)] *Deutsches Zentrum für Luft- und Raumfahrt (DLR)/Oberpfaffenhofen, Mobile Raketen Basis, Münchener Straße 20, 82234 Weßling, Germany, E-mail: marcus.hoerschgen-eggers@dlr.de*

[(3)] *ArianeGroup, Rue du Général Niox, 33165 Saint-Medard en Jalles Cedex, France, E-mail: gregory.pinaud@airbusafran-launchers.com*

[(4)] *ArianeGroup, Rue du Général Niox, 33165 Saint-Medard en Jalles Cedex, France, E-mail: maxime.podeur@airbusafran-launchers.com*

ABSTRACT

The application of aerospace thermal protection systems (TPS) is not limited to orbital flight and re-entry vehicles. Although less critical in terms of the thermal load's magnitude, it is also an essential part of sounding rocket primary structures.

For a large variety of launch vehicles, DLR's Mobile Rocket Base (MORABA) uses thermal protection systems on primary structures such as fin, nose cone, conical adapter and heat shield assemblies. Hereby, an ablative, epoxy based, two component thermoset coating has been the material of choice over several decades. Using relatively simple manufacturing methods, it can be sprayed onto almost any geometry. However, its noxious fumes released during the spraying process, its limited shelf life, its extensive storage requirements and above all, its residues polluting adjacent payload components during the ablation phase, are the key drivers for the development of a new thermal protection system using a special cork material.

This paper presents the development and manufacturing process as well as flight testing and post-flight analyses for different cork protected structural components flown on recent scientific missions (e.g. MAIUS 1, MAPHEUS 6, etc.). Results are discussed and a future outlook is given.

1 MOTIVATION

Aerospace thermal protection systems (TPS) are an essential part of sounding rocket primary structures such as fin, nose cone, conical adapter and heat shield assemblies; see also Fig. 1. Until recently the Mobile Rocket Base (MORABA) of the German Aerospace Centre (DLR) used an ablative, epoxy based, two component thermoset coating as TPS material.

Figure 1. IMPROVED MALEMUTE (IM) vehicle with cork based TPS on fin and motor adapter assemblies.

However, its noxious fumes released during the spraying process, its limited shelf life, its extensive storage requirements and above all, its residues polluting adjacent payload components during the ablation phase, are the key drivers for the development of a new thermal protection system.

2 TPS MATERIAL SELECTION

Besides the main functionality as a TPS material, the following additional requirements are considered as stringent for the selection of the new TPS material:

- Easy to apply on various shaped geometries,
- low mass,
- environmentally friendly (REACH, pollution of adjacent structures),
- low procurement and process costs,
- easy to store,
- easy to repair,
- good availability,
- preferably "Made in the European Union (EU)",
- no or less export restrictions.

From these outlined specifications resin infiltrated cork has been selected as the most potential TPS substitute. ArianeGroup (AG) 40 years of experience in the design, manufacturing and integration of cork based TPS for several space flight vehicles is a further key asset in selecting especially NORCOAT® LIÈGE HPK FI as the most promising semi-finished product available on the EU market.

NORCOAT® LIÈGE HPK FI is a low density thermal insulator based on cork granules mixed with phenolic resin as matrix; it is manufactured by LIÈGE HPK and marketed by AG. It is currently used on Ariane 5 launch vehicles, on M 51 French deterrence force missiles and has been successfully operated on the Atmospheric Re-entry Demonstrator (ADR) back cover as well as on the front heat shield of the BEAGLE 2 space probe of the European MARS EXPRESS mission. Furthermore, the successful operation on the latest Mars re-entry capsule Schiaparelli (EXOMARS mission, Fig. 2) proved the robustness of the material.
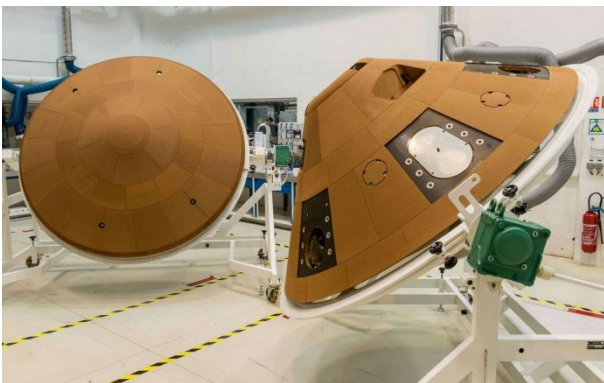

Figure 2. NORCOAT® LIÈGE HPK FI on the Mars re-entry capsule Schiaparelli; source: ESA.

NORCOAT® LIÈGE HPK FI is produced in form of flat plates of various thicknesses from 1.5mm to 19.0mm and can be further processed by e.g. machining (e.g. cutting, milling, etc.), hot-press forming, adhesive bonding and outgassing treatment for special space applications.

3 THERMAL ANALYSIS

In order to pre-assess the minimum TPS material thickness required as well as the charred layer thickness, a one-dimensional thermal analysis has been performed, considering a stacking of material and thermophysical phenomena as shown in Fig. 3.
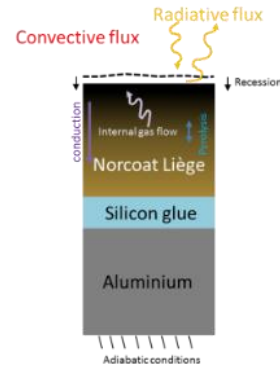

Figure 3. Schematic view of material and thermophysical phenomena stacking.

The simulation has been carried out on the VSB-30 aluminium forward nose cone (FNC) structure, laminated with 1.5mm as well as 2.0mm sheets of NORCOAT® LIÈGE HPK FI, using the commercial code AMARYLLIS (part of the SAMCEF code suite).

3.1 Method and Material Response Modelling

NORCOAT® LIÈGE HPK FI is a so called charring material, which decomposes when subjected to high temperatures, followed by a decrease in the material's density. Since this material consists of different constituents, its degradation can occur over different temperature ranges. To account for this type of behaviour, a multiple species Arrhenius definition can be used. However, for the herein described simulation only a single species Arrhenius law has been applied, due to available material model; Eq. 1.

$$\frac{\partial \rho}{\partial t} = -A \rho_v^{1-N} (\rho - \rho_c)^N e^{-\frac{E}{RT}} \tag{1}$$

The above described degradation results in the production of gaseous products, which diffuse through the material. Therefore the steady state gas mass balance equation is used; Eq. 2.

$$\frac{\partial \rho}{\partial t} + \nabla . \dot{m}^g = 0 \tag{2}$$

Assuming an ideal gas law, and introducing Darcy's law to relate the pressure of the gas to the gas mass balance, Eq. 3 can be formulated.

$$\overline{\dot{m}}^g = -K_P \nabla P$$
$$K_P = \frac{M^g \beta P}{\mu^g RT}$$

$$(3)$$

By introducing the pressure as a variable, a three-dimensional gas flow can be defined, using a scalar degree of freedom. Thus a direction of gas mass flow has not to be imposed beforehand. The heat balance equation reflects the time variation of enthalpy (both solid and gas), the heat conduction and the presence of gas in the pores of the solid parts. The model is set up with a local thermal equilibrium, assuming the gas and the solid parts having the same temperature at microscale. With the assumption of linear enthalpy variation, the following heat balance equation is obtained, Eq. 4.

$$-\frac{\partial \rho}{\partial t} H_p + \rho c \frac{\partial T}{\partial t} = -\nabla . \lambda \nabla T - \overline{\dot{m}}^g . \nabla h^g$$

$$(4)$$

All temperature dependent material properties (ρ, λ, c_p) are obtained by interpolation between the virgin and the charred state.

3.2 Loads and Boundary Conditions

The VSB-30 vehicle's ascent velocity, altitude and heat flux over flight time are applied and taken from TEXUS 43 nominal trajectory data; see also Fig. 4 and Fig. 5.
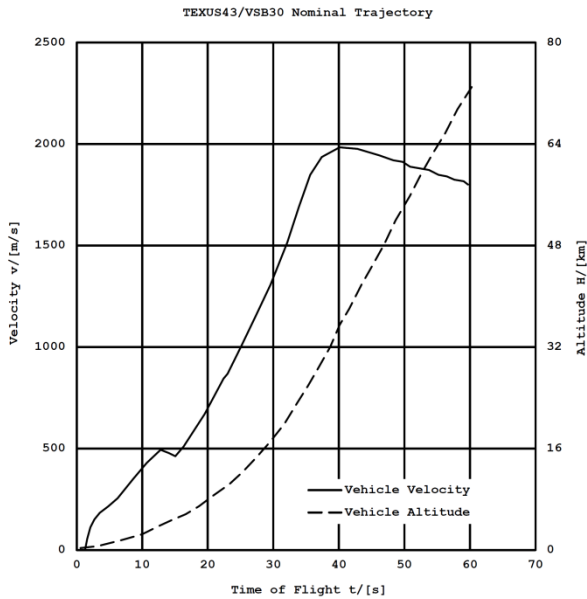

Figure 4. TEXUS 43 nominal vehicle velocity and altitude data.

Since the VSB-30 FNC structure is ejected after approximately T+60s the simulation is only carried out within this time frame.
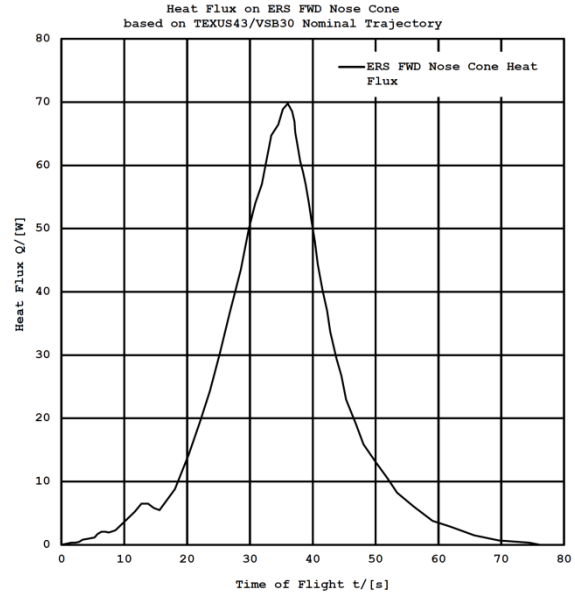

Figure 5. Heat flux on VSB-30 FNC base on TEXUS 43 nominal trajectory data.

The predicted cold wall heat flux is tabulated for different wall temperatures based on the trajectory data and is then rebuilt in an iterative loop.

In total three types of boundary conditions are applied to the model:

- The outer surface pressure, representing the aerodynamic pressure (Eq. 5),
- the outer wall temperature, dependent on the applied heat flux (convective and radiative term, Eq. 5),
- the imposed temperature dependent ablation speed (Eq. 6).

$$-\lambda \frac{\partial T}{\partial n} = q(T_w, \overline{x}, t) + \epsilon \sigma (T_r^4(\overline{x}, t) - T_w^4)$$

$$(5)$$

$$\dot{s} = \dot{s}(T_w)$$

$$(6)$$

The surface ablation is implemented by a moving ablation surface and a deforming volume.

3.3 Results

Fig. 6 shows the calculated FNC's inside wall temperatures for the different NORCOAT® LIÈGE HPK FI layer thicknesses (1.5mm and 2.0mm) and

typical inflight measured temperatures for a 1.0mm layer of the traditional epoxy based thermoset coating.
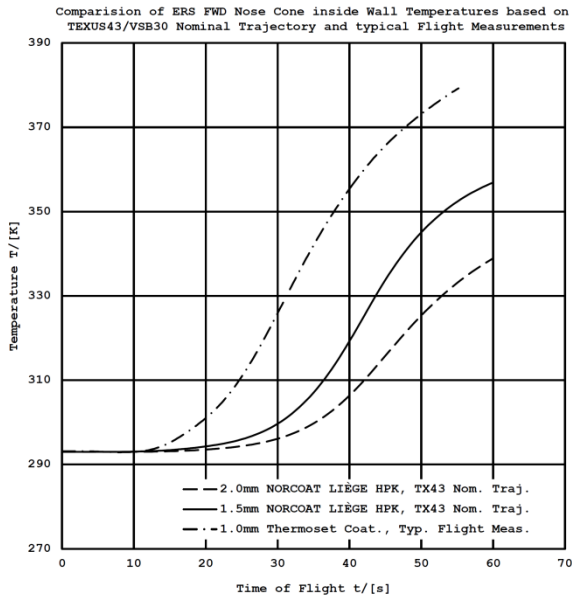

Figure 6. Comparison of predicted inside wall temperatures.

After T+60s, maximum inner wall temperatures of ~357K (84°C) for 1.5mm and ~338K (65°C) for 2.0mm of cork are reached. The resulting temperatures can be rated as non-critical compared to the measured temperature for the traditional epoxy based thermoset coating and to the maximum service temperature of the aluminium structure. However, a direct comparison of the cork and epoxy based thermoset TPS is not possible due to the different layer thicknesses applied.
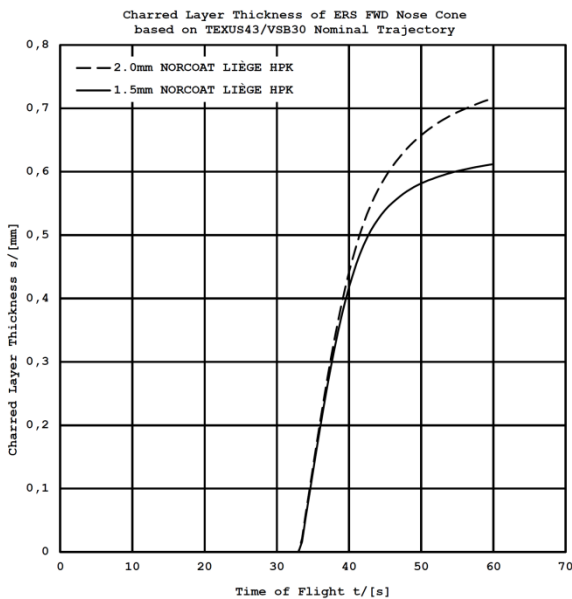

Figure 7. Comparison of TPS charred layer thicknesses.

Fig. 7 shows the calculated NORCOAT® LIÈGE HPK FI charred layer depth for virgin layer thicknesses of 1.5mm and 2.0mm. During the ascent phase the pyrolysis is expected to start from approximately T+30s and the TPS external surface to be fully charred. After T+60s the pyrolysis front can reach a depth of ~0.6mm for 1.5mm and ~0.7mm for 2.0mm virgin cork layer thicknesses.

Showing non-critical wall temperatures and non-sensitive insulation behaviour, a layer of 2.0mm NORCOAT® LIÈGE HPK FI has been selected as the VSB-30 FNC's TPS substitute for further manufacturing trails as well as inflight testing. Considering a 2.0mm coating and the respective adhesive layer, the total aerial mass at lift-off for this TPS solution would be less than $1.5kg/m^2$.

4 MANUFACTURING PROCESS AND HARDWARE

Another major part of the TPS substitution has been the development and establishment of a suitable manufacturing process by fulfilling the following main needs: Low process costs, less lead time, environmentally friendly, applicable to all TPS related structures, performable by 1-2 workers.

The essential process steps (Fig. 8) can be named in the right order as: Surface preparation, structural adhesive application, TPS layer application, vacuum bagging and curing, finishing.
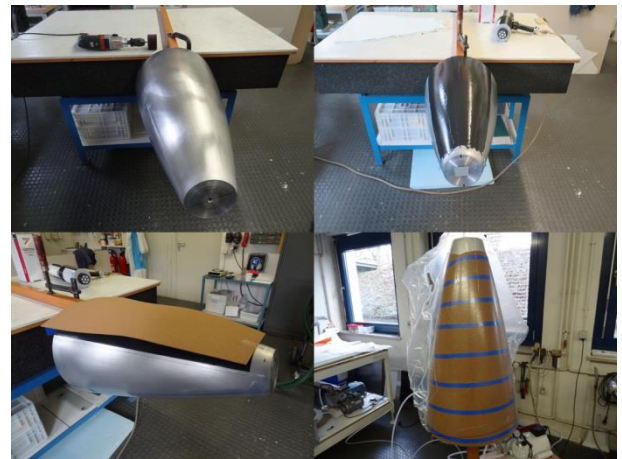

Figure 8. NORCOAT® LIÈGE HPK FI application on VSB-30 FNC structure.

After the successful manufacturing process development, performed on a VSB-30 FNC structure (Fig. 8), it has been adopted to other TPS related structures such as fin, motor adapter and heatshield assemblies (Fig. 9).
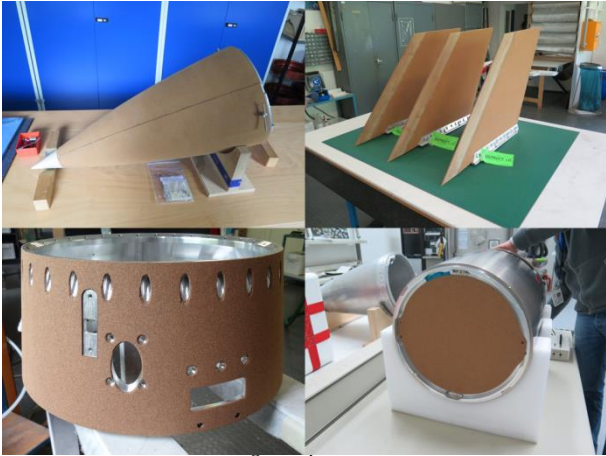
Figure 9. NORCOAT® LIÈGE HPK FI applied on various primary and secondary sounding rocket structures.

Up to present, this process is object of a continuing iteration loop of certain process parameters and thus of further improvements for serial production.

5   FLIGHT TESTING

With several flight hardware items coated using the cork based TPS, flight testing has been imminent.

The first NORCOAT® LIÈGE HPK FI coated structures tested during flight were fin and motor adapter assemblies for IM sounding rocket vehicles, launched for the MAXI-DUSTY missions in July 2016 from Andøya Space Centre in Norway. Due to the tight time schedule for the preparation of these missions none of these structures were instrumented with temperature or other sensors. However, measured trajectory as well as inflight video footage showed non-critical, nominal vehicle behaviour and thus the first operation of the new TPS material is considered as a success.

During the two follow-up missions MAIUS 1 in January 2017 and MAPHEUS 6 in May 2017, both launched from ESRANGE in Sweden, two cork coated FNC and heat shield assemblies were successfully flight tested on the VSB-30 vehicle. Each of the FNC assemblies was equipped with two PT100 temperature sensors.

Figure 10. MAPHEUS 6 in the Skylark tower (left), payload (mid) and cork coated FNC recovery (right).

Fig. 10 shows the cork coated FNC assembly launched on the MAPHEUS 6 mission, which could be fully recovered after the re-entry.

6   POST FLIGHT ANALYSES

The measured flight data from MAIUS 1 and MAPHEUS 6, as well as the recovered FNC structure flown on MAPHEUS 6, have been used for further post flight investigations described in the following subchapters.

6.1   Comparison of Flight Data

Before comparing the MAIUS 1 and MAPHEUS 6 measured temperature data, a closer look on the underlying trajectory data as well as the PT100 temperature sensor position and mounting technique is necessary.
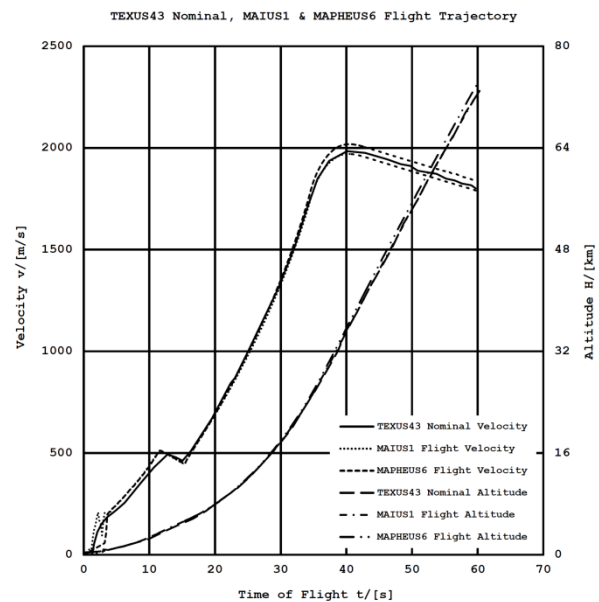

Figure 11. Comparison of TEXUS 43 nominal, MAIUS 1 and MAPHEUS 6 flight trajectory data.

Fig. 11 shows a comparison of the measured MAIUS 1 and MAPHEUS 6 trajectory data from lift-off until FNC separation (T+60s). The related measured vehicle velocity and altitude is plotted together with the TEXUS 43 nominal trajectory data, taken for the pre-asset thermal analysis. Apart from some minor deviations shortly after lift-off, the graphs show a good accordance and thus representing a reasonable basis for the temperature comparison.

Fig. 12 shows the standard positions and mounting technique of the two PT100 sensors (T1 & T2) on the inside of the FNC structure as integrated on the MAPHEUS 6 flight hardware. The sensor itself was casted inside an aluminium casing (Fig. 12, bottom, left)

and bonded on the respective position on the inside of the aluminium structure (Fig. 12, bottom, right) using a high temperature conductive resin.
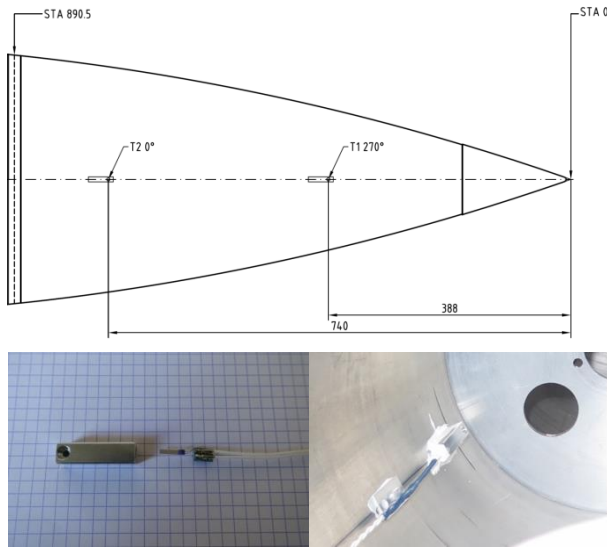

Figure 12. Position and application of PT100 sensors.

In contrast to MAPHEUS 6, the MAIUS 1 FNC was of a spherically blunted geometry (90mm tip radius) and ~200mm shorter in length. Both PT100 sensors were mounted close together at the T2 position (measured from the separation interface STA 890.5). The reason for this application was to evaluate the influence of one sensor mounted with and one sensor without the aluminium casing.

Fig. 13 shows the measured inside wall temperatures of MAPHEUS 6 and MAIUS 1 together with the predicted temperatures from the pre-asset analysis over the first 60s in flight. In general, the measured temperatures are clearly below the predicted ones. The MAIUS 1 T2 sensor without the aluminium casing measured the highest and the closest values to the prediction (~14% max. deviation). Because of its higher thermal mass, all sensors casted in the aluminium casing showed a clear delay and thus ending up with much lower magnitudes at the point of nose cone separation (~50% max. deviation). Due to the different ambient temperature conditions at launch, a clear difference of the measured values between MAIUS 1 and MAPHEUS 6 is detected. However, assuming a similar heat capacity for both nose cone structures, a comparison of the various temperature differences from lift-off until nose cone separation is feasible.

By comparing the MAPHEUS 6 T1 sensor to its T2 sensor only a marginal difference (<10% max. deviation) can be detected resulting from the different sensor positions.
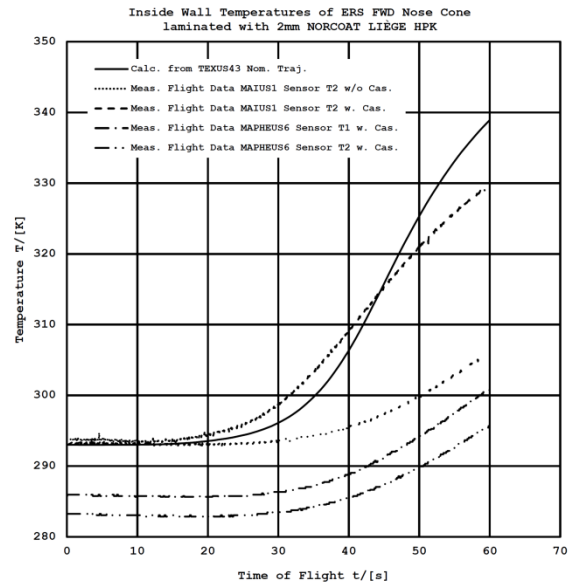

Figure 13. Comparison of measured and calculated inside wall temperatures.

Negligible, small deviations can be found by comparing the T2 sensor of MAIUS 1 to the T2 sensor of MAPHEUS 6, implying only small deviations at T2 position due to the different nose cone geometries.

6.2 Recovered Flight Hardware Inspection

In addition to the post flight analysis of measured data an investigation of the recovered MAPHEUS 6 FNC structure has been performed. Besides the first visual inspection, five samples have been cut out from various nose cone positions (including the T1 and T2 positions), prepared and inspected under a light microscope.
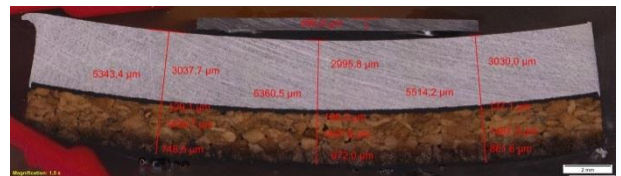

Figure 14. Light microscopic investigation of MAPHEUS 6 FNC cut-out samples.

Fig. 14 shows the light microscopic picture of the sample cut out at 650mm from the nose cone separation plane. For all samples the stacking has been measured and the average thicknesses can be summarised as follows:

- Adhesive layer   0.15mm,
- virgin cork layer   1.80mm,
- charred cork layer   1.10mm,
- total cork layer   2.90mm.

From the original and measured total cork layer thickness an approximate swelling of ~45% can be calculated.

In addition to the material thicknesses, the microscopic pictures also revealed a very high porosity of the sensor casting inside the aluminium casing as well as of the bonding layer between the nose cone structure and the aluminium casing.

6.3 Thermal Analysis Validation

In order to get a better insight of the deviation between calculated and measured temperatures, a validation of the thermal simulation has been carried out and is described in this subchapter. Furthermore, this validation has been only performed on the example of the MAPHEUS 6 flight hardware, since the FNC geometry flown on the MAIUS 1 mission is not representing the standard tip geometry.

6.3.1 Actual Trajectory and Atmospheric Data

The measured MAPHEUS 6 main trajectory parameters together with the actual atmospheric profile have been used to rebuild more realistic aerothermal loads for the heat flux calculation. Since all weather balloons, launched during the countdown, were measuring exclusively wind speed and wind direction, only forecasted atmospheric profiles have been used.

6.3.2 Aerothermal Loads Assessment

For the assessment of the aerothermal heat flux the software ARPEGE, coded by Airbus, has been selected. ARPEGE (Aérothermodynamique de Rentrée pour PrédirE la fraGmentation d'Etages) is a fast computer programme designed to predict surface pressure, shear stresses, aerodynamic forces, coefficients and heat transfer distributions of an arbitrary shaped geometry at hypersonic speed. Below 40km (until T+40s) the VSB-30 vehicle is not strictly in a hypersonic regime, however for a first quick assessment the tool is considered as sufficiently accurate.

The MAPHEUS 6 FNC geometry has been used to create a three-dimensional surface mesh. Furthermore, a zero degree angle of attack is assumed all along the trajectory leading to an axisymmetric heat flux distribution.

Fig. 15 shows the resulting cold wall aerothermal heat flux distribution at T+35s for a uniform initial temperature of 300K. At high Mach numbers the heat flux profile decreases rapidly after a few centimetres measured from the nose tip.
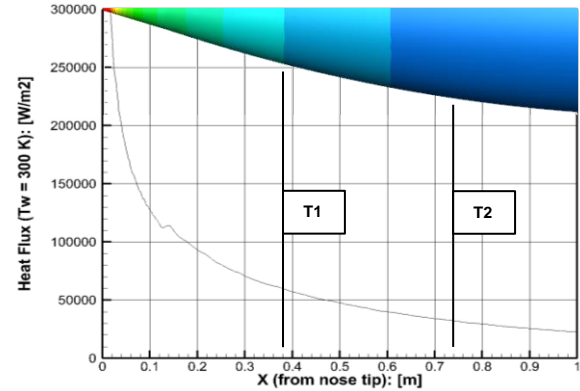

Figure 15. MAPHEUS 6 calculated cold wall aerothermal heat flux profile at T+35s.

At each point of the recorded trajectory, steady state runs provide the time profile of the heat flux on any location of the FNC.
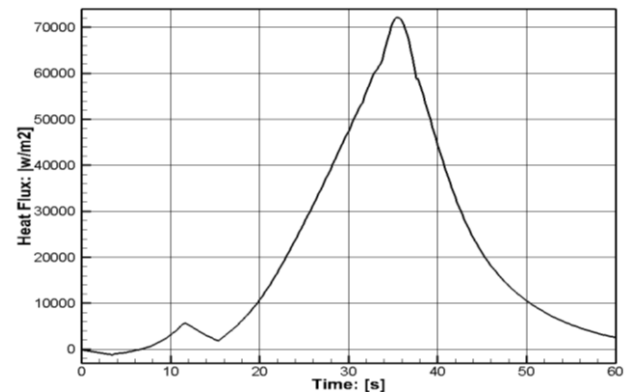

Figure 16. MAPHEUS 6 calculated cold wall aerothermal heat flux time profile (300mm from the nose tip).

Fig. 16 shows the time profile of the aerothermal heat flux at the exact location of the temperature sensor T1, which is similar to the initial heat flux taken for the pre-asset analysis (Fig. 5). However, an over prediction in the subsonic and low supersonic regime must be considered due to the described limitations of the ARPEGE programme.

6.3.3 Thermal Response Assessment

Based on the microscopic investigations, as well as on the PT100 sensors actual integration and mounting situation, a more realistic material stacking has been taken into account. Therefore, a three-dimensional model, including a numerical thermocouple with aluminium casing, has been created. The simulation has been performed using the same software (AMARYLLIS), method and boundary conditions as used for the one-dimensional pre-asset analysis described in chapter 3. Finally, for the calculation of the temperatures at the T1 and T2 positions the previously

calculated time-dependent aerothermal heat fluxes of these respective locations have been applied. For the material input the actual parameters of all materials used have been taken from corresponding technical data sheets.
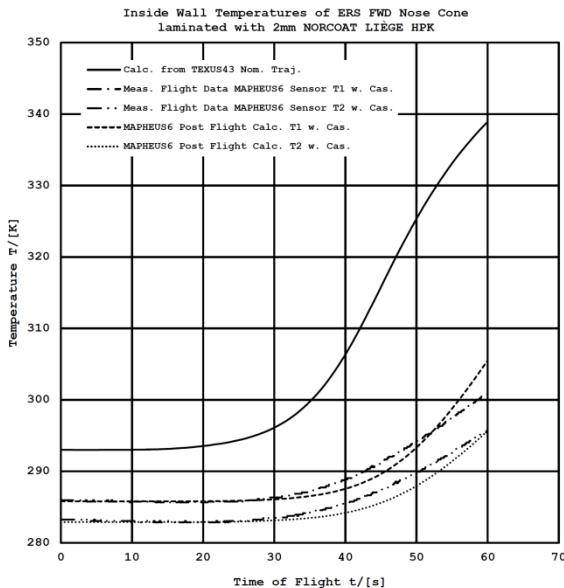

Figure 17. Comparison of measured, calculated and validated inside wall temperatures.

Fig. 17 shows the inside wall temperatures of the pre-asset calculation as well as those measured during the MAPHEUS 6 flight and those from the validation runs. Although the initial temperature of the pre-asset calculation is slightly higher, a comparison of the various temperature differences from lift-off until T+60s is feasible. Thereby, the validated results show a clear trend towards a more accurate temperature prediction. However, their steeper gradients are still indicating a different behaviour and thus the data shall be handled with care. One major aspect concerning the different temperature gradients is linked to the pour quality of the casting and mounting of the respective temperature sensors.

The predicted charred layer thickness resulting from the pyrolysis (Fig. 18) has been compared to the cut-out samples from the recovered MAPHEUS 6 FNC (Fig. 14) and has been proved as consistent with the observations.

Because of the relatively low convective heat flux during the vehicle's ascent phase, the simulated temperatures remain below the ablation threshold. Consequently, the simulation did not predict any surface recession.

Due to the model's simplifications, swelling is not directly considered. Instead, the apparent diffusivity is corrected on the basis of a comprehensive infra-red and plasma internal test.
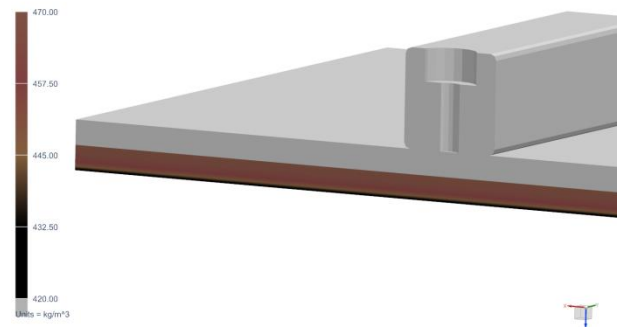

Figure 18. Simulated charred layer thickness after the VSB-30 ascent phase.

7 SUMMARY AND LESSONS LEARNED

The herein described work can be summarised as follows:

- NORCOAT® LIÈGE HPK FI has been pre-selected as a suitable cork based TPS substitute for various sounding rocket primary and secondary structures.

- A pre-asset one-dimensional thermal analysis has been performed for the VSB-30 FNC using 1.5mm and 2.0mm thick NORCOAT® LIÈGE HPK FI layers. Non-critical structural heating has resulted from this investigation.

- A suitable manufacturing process using 1.5mm and 2.0mm thick NORCOAT® LIÈGE HPK FI layers has been established for various sounding rocket primary and secondary structures.

- Various sounding rocket primary and secondary structures such as fin, motor adapter, nose cone and heat shield assemblies have been flight tested on four different missions.

- A post flight investigation of on-board measurements and recovered hardware has been performed for the VSB-30 FNC structure.

- A post flight validated three-dimensional thermal analyses has been carried out, leading to an improved predictability of the structural heating as well as the ablation process of the cork based TPS.

For a more detailed understanding of the phenomena and a more accurate prediction of the structural heating as well as the TPS ablation the following lessons learned can be named:

- In order to enlarge the set of flight data, future comparable flight hardware items should be equally

equipped with temperature sensors and data should be monitored.

- The temperature sensor mounting technique should be improved to ensure a reliable data acquisition, especially without the sensor's aluminium casing and a professional sensor bonding technique.

- A complete atmospheric profile should be measured by atmospheric balloons during the countdown and thus providing better input for the post flight analysis.

- A full uncertainty analysis of the input parameters should be performed to understand the sensitivity of the simulated results.

- A more adequate analysing method for the computation of the heat flux, especially for the subsonic and low supersonic regime, should be applied.

- The ablation and swelling behaviour should be investigated more deeply. Therefore, a more advanced hardware recovery and sample preparation procedure is necessary (e.g. charred layer fixation after landing).

ACKNOWLEDGEMENTS

REFERENCES

[1] A.J. van Eekelen, J.-M. Bouilly, S. Hudrisier, J.-M. Dupillier and Y. Aspa. Design and Numerical Modelling of Charring Material Ablators for Re-entry Applications. In 6th European workshop on Thermal Protection Systems and hot structures, April 2009, Stuttgart.

[2] G. Pinaud, Thermo-chemical and mechanical coupled analysis of swelling charring and ablative materials for re-entry application, 5th AF/SNL/NASA Ablation Workshop, Lexington (KY), 2012

[3] G. Pinaud, Thermo-chemical and mechanical coupled analysis of swelling charring and ablative materials for re-entry application, 5th AF/SNL/NASA Ablation Workshop, Lexington (KY), 2012